Post-lithium-ion battery cell production and its compatibility with lithium-ion cell production infrastructure

Fabian Duffner[a,b*], Niklas Kronemeyer[b], Jens Tübke[c], Jens Leker[a,e], Martin Winter[d,e], and Richard Schmuch[d*]

[a] University of Münster, Institute of Business Administration at the Department of Chemistry and Pharmacy, Leonardo-Campus 1, 48148 Münster, Germany

[b] Porsche Consulting GmbH, Porsche Straße 1, 74321 Bietigheim-Bissingen, Germany

[c] Fraunhofer Institute for Production Technology, Forschungsfertigung Batteriezelle FFB,

[d] University of Münster, MEET Battery Research Center, Institute of Physical Chemistry, Corrensstr. 46, 48149 Münster, Germany.

Mendelstraße 11, 48149 Münster, Germany.

[e] Helmholtz Institute Münster, IEK-12, Forschungszentrum Jülich GmbH, Corrensstr. 46, 48149 Münster, Germany.

[*]Corresponding authors:

Dr. Fabian Duffner

fabian.duffner@uni-muenster.de

Dr. Richard Schmuch

richard.schmuch@uni-muenster.de

Lithium-ion batteries (LIBs) are the currently most advanced electrochemical energy storage technology due to a favorable balance of performance and cost properties. Driven by forecasted growth of the electric vehicles market, the cell production capacity for this technology is continuously being scaled up. However, the demand for better performance, particularly higher energy densities and/or lower costs, has triggered research on post-lithium-ion battery technologies such as solid-state lithium-metal, lithium-sulfur, and lithium-air batteries as well as post-lithium technologies such as sodium-ion. Currently, these technologies are being intensively studied with regard to material chemistry and cell design. This article reviews and expands the current knowledge in this field. Starting with a market outlook and an analysis of technological differences, we discuss manufacturing processes of those technologies. Anode production, cathode production, cell assembly, and conditioning for each technology are described. Then, the manufacturing compatibility of each technology with the lithium-ion production infrastructure is evaluated and implications on process costs are discussed.

Rechargeable batteries have a long history of technology development, starting with the expansion of lead-acid technology to commercial scale around the year 1860. Since then, several secondary battery technologies have been commercialized including manganese dioxide-zinc, nickel-cadmium, nickel-

metal hydride and lithium-ion batteries. The commercialization path has resulted in enormous performance improvements. Lead-acid batteries (LEAs), which today still dominate the automotive starter sector can achieve gravimetric energy densities of 20 to 40 Wh kg^{-1}, while the first-generation of LIBs introduced in 1991 had already reached 80 Wh kg^{-1} [1,2]. At the early stage of LIB technology, achievements in energy density were accompanied by cost drawbacks. Since then, the cost of LIB cells has decreased to less than 150 US$ kWh^{-1} [3] and energy density has further increased to more than 250 Wh kg^{-1}, making LIBs the prevalent high energy density technology.

Driven by this technological evolution, various industries began using LIBs for energy storage. Today, LIB technology is already in widespread use in mobile electronic devices (e.g., phones, tablets and laptops), electric bicycles, e-scooters, power & gardening tools and forklifts[4]. In addition, it is likely that LIB-powered electric engines will (partially) displace the combustion engine as the leading propulsion technology in the automotive sector in the mid-term and will support fuel cell drive trains in the future. In 2019, the LIB battery manufacturing market accounted for >160 GWh $year^{-1}$ of a total rechargeable battery market of >600 GWh $year^{-1}$ (Fig. 1). Especially driven by the increasing market share and the high energy content per electric vehicle application (on average 10 kWh $vehicle^{-1}$ for hybrids and 68 kWh $vehicle^{-1}$ for full battery electric vehicles[5]) this capacity is forecasted to increase to 1,500 GWh $year^{-1}$ by 2030 (Fig. 1). Driven by this increase in capacity, billions of dollars will be invested in the manufacturing infrastructure (see Table 1) for the respective state-of-the art battery cell technology (currently LIB).

Increasing demand has led to the set-up of numerous new LIB cell factories. However, due to current requirements especially for further cost reduction and increased energy density, alternative battery technologies beyond the LIB are being intensively discussed. Based on their theoretical energy contents, several, so-called post-lithium-ion-batteries (PLIBs) promise higher gravimetric and volumetric energy densities compared to LIBs (Fig. 1), for some technologies even being forecasted to exceed 1,200 Wh kg^{-1} and 800 Wh L^{-1}. In addition, they promise cost advantages[5–8], which is in many cases rationalized with lower raw material costs of the cell components (e.g., sodium[5], sulphur[9] and oxygen) or optimized cell component concepts (e.g., anode-free batteries[10,11]). Table 2 provides an overview of the key (dis-)advantages as well as technical specifications of the discussed battery technologies, while Figure 2 shows the corresponding active material configurations as well as stacking of cell components. While many PLIB technologies are being produced at lab or pilot scale, currently no studies on their series manufacturing exists.

This article examines industrial-scale manufacturing of LIBs and four commonly discussed PLIB technologies: sodium-ion batteries (SIBs) and the lithium-metal based batteries, namely lithium-sulfur batteries (LSBs), solid-state batteries (SSBs), and lithium-air batteries (LABs). These PLIB technologies were selected for the following reasons. SIBs are being widely regarded as an alternative, drop-in technology for LIBs and might gain importance, in case limited resources, such as limited lithium supply should become an issue in the future. The three Li-metal based PLIB technologies promise high energy contents and are being anticipated on the battery technology roadmaps worldwide. LSBs could not yet been commercialized successfully at a large scale, despite the steady increase of their specific energy (currently >400 Wh/kg_{cell}) through optimization of electrode architecture and minimizing electrolyte excess. They are thus likely to be constrained to specialized applications such as aviation. In recent years, the highest hopes to advance beyond LIBs have been associated with SSBs, whose major advantages would lie in higher energy contents (>350 Wh/kg_{cell}) through the implementation of lithium metal and enhanced safety by replacing the flammable liquid electrolyte with a non-flammable solid

electrolyte. In spite of intense efforts by many researchers, all reported SSBs regardless of whether they use a polymer, an inorganic (sulfidic or oxidic) or a hybrid electrolyte version of the three, to date still fall short of electrochemical performance (energy, power, life) in comparison to LIBs[12]. However, from a manufacturing perspective, polymer-based SSBs can be industrialized in a similar way like conventional LIBs[10], whereas the industrialization of sulfidic and oxidic SSBs is much more challenging and requires new manufacturing machinery, competencies and environments and is thus focused within this article. LABs are associated with the most difficult technical challenges, including pore clogging of the air electrode during operation, their potentially attainable energy content is also most appealing (currently depending on the calculation basis >1.200 Wh/kg_{cell})[13] and have thus been included in this study. Other alternative battery chemistries (*e.g.* aqueous LIBs) were not included in this work, as they presently do not offer sufficient advantages (*i.e.*, energy density, raw material availability, life) over current batteries and thus are not expected to qualify for a broad market.

In the following, we first compare the battery technologies, focusing not only on their strengths and weaknesses with regard to performance and cost, but also on the used materials, cell designs, as these have considerable impact on the cell manufacturing processes. Finally, we describe the manufacturing steps for each technology, evaluate the implication of a technology leap for existing lithium-ion cell production facilities, and discuss the implications on processing costs.

Architecture of selected rechargeable battery technologies

In this section, materials and cell designs of the current LIB technology as well as of four emerging battery technologies are briefly described. PLIBs are discussed in reference to the specifications of LIB technology, which currently represents the state-of-the-art. While LIBs and SIBs rely on intercalation chemistry, LSBs, SSBs and LABs involve a shape-changing lithium metal anode, which is deposited/stripped during each charge/discharge cycle. With regard to raw material costs per kg (material level) and raw material availability, individual components of SIBs show advantages over LIBs, which however do not result in lower costs per energy (US$ kWh^{-1}) at cell level[5]. While PLIB technologies such as LSBs or LABs involve potentially low-cost cathodes, their lithium metal negative electrode, which often involves a large lithium excess, might significantly increase raw material and processing costs. Estimated cost for unprocessed lithium metal (ingot) amounts to 50-130 US$ kg^{-1} [14], whereas cost of battery-grade lithium carbonate or hydroxide ranges from 8-11 US$ kg^{-1} [14].

Lithium-ion battery technology: Major constituents of a LIB are the cathode (positive electrode)[15] and the anode (negative electrode)[16] as well as the separator and the electrolyte. Layered (transition) metal oxides ($LiMO_2$ with *M* = Ni, Mn, Co and/or Al), are the most widely used class of positive active materials[17], while artificial and natural graphites are mostly used as negative active materials[14,18,19]. Key inactive components include aprotic liquid electrolytes with lithium salt, thin microporous, polyolefin-based separator films (~20 µm)[20] and sheets of aluminium (~12 µm) and copper (~8 µm) are used as current collectors for cathode and anode.

Sodium-ion battery technology: SIBs have the same fundamental working principle as LIBs, but rely on sodium rather than lithium as mobile cations. Unlike lithium, sodium does not electrochemically alloy with aluminium at room temperature. Thus, the copper current collector or the negative electrode can be replaced by cheaper aluminium. Hard carbon is typically used as anode active material instead of graphite, as crystalline graphite has poor storage capabilities for sodium ions[21,22].

Electrolytes and separators as well as the positive current collectors are similar to LIBs, except for using sodium salts in the electrolyte.

Lithium-sulfur battery technology: LSBs use nanostructured sulfur/carbon composites with high amounts of conductive carbon as positive active material, while lithium metal is used as negative active material. Since their operation relies on soluble polysulfide species within the electrolyte[23], high amounts of electrolyte are necessary, which reduce the practically attainable energy density.[7,24]

Solid-state lithium metal battery technology: High-energy SSBs use a lithium metal anode and a composite cathode, which consists of the cathode active material, (optionally) a conductive additive, and a certain mass/volume fraction of a solid electrolyte (SE)[12]. Ideally, the SE simultaneously acts as an ionic conductor and electronic insulator[25], which enables the SE to also act as separator film[26,27]. Ideal SEs can suppress lithium metal dendrite formation and growth. Various inorganic ceramics or lithium salts in organic polymers are suitable for the SE. Inorganic ceramics can be further differentiated into sulfides and oxides[10,25,28], which are both in the focus of the following section on manufacturing.

Lithium-air battery technology: The architecture of LABs differs fundamentally from all previously discussed battery types, as LABs involve the use of oxygen as a gaseous positive active material, which ideally could directly be taken from atmosphere[13,29]. LABs use an oxygen- or air-permeable carbon cathode with a porosity of around 80%[30]. To ensure sufficient oxygen supply, cathode grids are used as collectors. Lithium metal is used as negative active material. Both aqueous and non-aqueous electrolyte formulations may be utilized, with the latter preferred due to their better stability against lithium metal[30,31]. Major technical challenges in development of LABs exist. Due to the presence of other atmospheric gases in air (i.e., N_2, CO_2 or H_2O), unwanted chemical products such as Li_3N, Li_2CO_3 or LiOH may form in the cathode[29], which negatively affect the attainable cycle life[32–34]. A promising approach to improve the cycling stability of LABs is the usage of an oxygen-selective membrane, which suppresses side reactions[30]. Compared to the previously described battery technologies, a new cell-stacking architecture is needed to ensure a sufficient supply of oxygen to the cathode, which could reduce cost and result in energy-density advantages at the system level[29]. Before the LAB technology can be scaled up, it is necessary to resolve fundamental issues regarding cell design and materials chemistry.

Manufacturing of selected rechargeable batteries technologies

Research on manufacturing of battery cells is gaining momentum. Most studies focus on the lithium-ion technology with the target to optimize process parameters. To achieve these improvements, a detailed understanding of the numerous consecutive and interacting process steps is mandatory[35,36]. However, beside the optimization of LIB manufacturing, the manufacturing of PLIBs must be focused within research activities, as it will require new process technologies, new manufacturing environments and new manufacturing competencies. Consequently, this section describes the manufacturing of LIB technology as well as selected PLIB technologies as illustrated in Figure 3, highlighting the differences of the manufacturing routes. For that, process steps are divided into three superordinate main processes: electrode production (anode and cathode), cell production, and cell conditioning. In addition, for SSBs, solid electrolyte production is discussed in detail, as in contrary to their liquid counterparts, parts of the SE are mixed with the cathode active material slurry to achieve ionic conductivity and SE is integrated as additional layers within the cell stack. Thus, electrolyte

production within SSBs requires a significantly higher processing effort compared to technologies with liquid electrolyte.

Anode production: For graphite and hard carbon negative electrodes used in LIBs and SIBs, in general the same production process is followed. First, the active material (graphite or hard carbon), binder (e.g., poly(vinylidene difluoride) (PVdF)), conductive additive (e.g., carbon black) and processing solvent (e.g., NMP, water), are typically mixed batch-wise (e.g., by planetary mixer) or continuously (e.g., by screw extruder[37,38]) to produce the anode active material slurry[5,14,39,40]. Where optimal homogeneity of the slurry is crucial to achieve desired cell performance (especially rate capability and electrode conductivity)[41], from a processing perspective, optimal slurry-viscosity is most relevant. In general, thin slurries allow for faster processing in the consecutive coating process but induce coating thickness variations and higher cost for solvents and subsequent drying[42]. To achieve optimal slurry properties within minimum processing time, various suspension strategies are available which sometimes use an upstream dry mixing procedure (e.g., by low-intensity dry homogenization) to blend active material, conductive additives and binder (optionally)[35]. Consecutively, thin metal carrier foils (Cu ~8µm; Al 12 µm)[43] are coated continuously or intermittent on both sides (e.g., by slot-die coating) and dried (e.g., by convection or infrared) to solidify the slurry by evaporating the solvent. Where currently typical coating speeds range between 25 and 50 m min^{-1} [35], future speeds of up to 100 m min^{-1} are targeted. To materialize this higher coating speed from a technical perspective, the bead pressure, the low-flow limit and its associated parameters must be controlled especially to avoid film break-ups and to ensure film uniformity as a basis to not deteriorate scrap rate and/or cell performance[44–46]. Further, dryer processing capacity must be improved to similar extent. Therefore, beside the strategy of increasing dryer length, the usage of infrared instead of convection dryers and optimized drying protocols are promising approaches[47,35]. To reduce porosity, the coating is then compressed by calendering in the next step. When the working width of the coater (up to 1.5 m) exceeds the width of a desired single anode sheet, anodes are slit to the desired width (e.g., by roll-knife or laser). Finally, the cathodes are dried (e.g., batchwise under vacuum or continuously under infrared) prior transfer to a dry room[35,48,49]. The described liquid suspension and web coating-based anode production for SIBs and LIBs represents the current state-of-the-art process. With regard to the future, various solvent free concepts are intensively researched as they promise cost advantages due to the elimination of the drying procedure (see Fig. 4).
Lithium metal anodes are typically used in SSBs, LSBs and LABs[25,30]. While lithium compounds such as Li_2CO_3 or LiOH are sufficient for cathode active material production of LIBs and SSBs, lithium anode production requires metallic lithium. To produce metallic lithium, purification and reduction by energy-intense electrolysis is necessary[50]. As metallic lithium is highly reactive with components of ambient air (oxygen, nitrogen, carbon dioxide, moisture)[51], it must be processed in inert gas atmosphere, typically argon[10].

As illustrated in ure 5, a typical lithium metal anode production comprises the following steps: First, lithium metal is extruded to form the ductile material into foil shape. Second, high-intensity calendering further reduces foil thickness. The high-intensity calendering process for lithium metal differs from conventional calendering of graphite anode. Conventional calendering reduces material thickness by reducing its porosity. As metallic lithium is non-porous and significantly lower thicknesses of 10 to 20 µm are targeted (compared to 50 to 150 µm in conventional anodes)[14], the number of operations and typical line loads of 500 N mm^{-1} used for calendering graphite anodes[35] are significantly exceeded. Further, the adhesive properties of lithium[51] must be controlled during calendering to avoid scrap. Third, the lithium foil is laminated on both sides of the current collector foil[10]. Prior transfer of the lithium metal foil out of the protective argon atmosphere, its surface must be passivated[14] to

conduct consecutive manufacturing steps under dry room conditions. For passivation, multiple approaches are available: gas treatment, coating layer of polyethylene wax or surface fluorination[52]. This passivation is necessary from a manufacturing perspective. Nevertheless, the passivation layer can in addition act protectively to suppress lithium metal dendrite formation/growth, and to suppress reaction of lithium metal with electrolyte which would result in reduced cell performance due to electronic conductivity and/or decompensation[8,25]. However, since protection concepts relying on additional layers (using e.g., polymers , ceramics , inorganic-organic composites or porous carbons)[53] cause drawbacks in terms of energy density and costs, strategies to produce this protective interlayer in situ via conversion reaction[54] or its complete omission by usage of materials which are mutually stable seem to be more advantageous. For example, within SSBs, this protective interlayer can be omitted in case of typically garnet structured oxidic SE, which are stable against lithium-metal and do not show any reaction in cyclovoltammograms up to 8V[8,55]. However, typical sulfidic SEs (e.g., LiGePS or LiSiSnPS) are not stable against lithium metal, as they include transition metal ions like Ge or Sn and thus, an interlayer protection is mandatory[8,55]. Beside the approach of finding an electrolyte that is stable against lithium metal, the usage of lithium alloys (e.g. Al, Ga, In, Sn, or Sb) as active material are discussed intensively since insertion of lithium into metal lowers electrolyte reduction while allowing lithium-ions to transfer into the electrode material[56]. After passivation, the mother coil is laser-slit to single electrodes or daughter coils. Mechanical roll-knife slitting, which is the established process for LIBs, is not suitable, due to the adhesive properties of lithium. Currently, lithium foil thicknesses of ≤15 µm cannot be produced at competitive costs. Thus, optimized processing techniques such as melt processing or vapour deposition are being discussed. As an alternative approach, so-called 'anode-free' concepts are considered, which involve lithium plating onto a pristine lithium-free current collector upon initial charge[10,11,57], rendering the elaborate production and processing of lithium metal foil unnecessary. To put this concept into practice, the necessary lithium must be provided by a lithium-containing cathode material.

Cathode production: Cathode production for LIBs, SIBs, and LSBs involves basically the same process steps as graphite and hard carbon anode production.

SSB composite cathodes are produced by using (1) a current collector foil, (2) an active material, (3) an SE and (4) a conductive additive. First, for the production of sulfidic and oxidic SSBs, active material slurry and SE slurry are mixed separately (e.g., by planetary batch mixer or permanent extruder). Second, as ionic conductivity within a battery cell is achieved by sufficiently connecting active material with electrolyte particles, part of the SE must be mixed with active material slurry (~30 vol% SE[8,10]). Accordingly, ionic conductivity within SSBs can be characterized by slurry homogeneity, which makes the composite mixing process step crucial for cell performance. Third, the composite slurry is coated (e.g., by slot-die-coating) onto an aluminium current collector foil. After coating, the consecutive process steps differ for cathodes with oxide- and sulfide-based SEs, mainly because the more brittle oxidic SEs (e.g., LLZO, $Li_7La_3Zr_2O_{12}$)[59] require production processes with lower mechanical stress.

Within sulfidic SSB production, after composite coating, the pure sulfidic electrolyte slurry is coated (e.g., by slot-die-coating) on top of the composite layer forming a cathode-electrolyte-assembly. Thereafter (and sometimes also before), the slurries are dried (e.g., by convection, infrared, or vacuum). After this step, the cathodes are calendered and slit. This might require advanced instrumentation and/or multiple calendering operations. Finally, a slitting process step is conducted, which is comparable to those used for LIB production and can be executed with a role-knife procedure. With regard to the production environment, cathode production of sulfidic SSBs must be conducted in

a dry environment (<100 ppm of H_2O[60]) or inert gas atmosphere, as the currently most promising class of sulfidic SEs is prone to ambient moisture, generating harmful H_2S[61–63].

While the described liquid suspension coating and calendering procedure is suitable to achieve targeted interfacial contact and porosity within the ductile sulfidic electrolyte, they are not sufficient to process the hard and brittle oxidic SEs[8]. Therefore, within oxidic SSB production, after composite slurry coating (e.g., by slot-die-coating), a low temperature pre-sintering step is conducted by which the particles of the composite cathode are connected and the intergrain ionic resistance is reduced[64]. In general, high temperature sintering (around 1000 °C) is not applicable as it leads to reaction of SE and active material resulting in disadvantageous products. For example, the typical active material LNMO and the typical SE LLZ decompose at 600 °C [8,65]. The sintering operations are ideally conducted in large-scale manufacturing by using efficient permanently operational sintering ovens. After sintering, cathode sheets of the oxidic SSB must be processed in dry room or inert gas atmosphere, as oxidic SEs would react with humid air and form Li_2CO_3 on the surface, resulting in decreased ionic conductivity[8,66]. Thereafter the composite cathode is slit and laser-cut into single sheets. In order to form the cathode-electrolyte-assembly, concepts exist to either produce the SE layer separately or to apply it directly onto the composite cathode. Within the first concept, the solid electrolyte layer is formed by coating the solid electrolyte slurry (solid electrolyte, binder, additives, solvent) on a carrier tape and the solvent is evaporated. Afterwards the sheets are cut to single sheets, which must be conducted by laser, as mechanical cutting processes are not suitable for the brittle oxidic SE layer. Thereafter a high temperature sintering operation at over 1000 °C for several hours is conducted[8]. Finally, the solid electrolyte is laminated onto the composite cathode layer and a further low temperature sintering operation is conducted. While this process chain seems feasible for small format layers (e.g., 2 x 2 cm^2), the upscaling to larger formats within industrial processes is a key challenge within commercialization of oxidic SSBs. Therefore, alternative concepts are discussed. Herein aerosol deposition is a potential technology in which solid electrolyte powder is applied directly to the composite cathode layer by using a carrier gas and is then compounded in a tempering step (e.g., 600°C)[67].Using this concept would enable the production of thinner electrolyte layers. Further, various process steps including time and resource-consuming sintering could be avoided. Nevertheless, the technology is in an early stage and especially deposition rates, which are currently limited to 10 mm^3 min^{-1}, must be improved e.g. by using multi-nozzle systems with broad nozzles for competitive industrial application[68].

Cathode production of LABs is crucial, as the structure of the cathode affects the overall battery performance to a significant extend, due to its impact on cathode material utilization, the morphology of the discharge products, the oxygen permeability, the ionic transfer and the electric conductivity[69]. High-performance LAB cathodes have a durable porous structure containing optimal pores (size and distribution) to store the discharge product and to provide sufficient oxygen supply[70,71]. Beside an optimal pore structure, it is crucial to avoid moisture uptake by the high-surface-area carbon black during production, as moisture blocks the deposition of the Li_2O_2 discharge product, thereby reducing capacity. Minimum moisture can be reached by solvent-free production in a dry atmosphere, which is currently being intensively studied for LIBs as well[72,73]. In solvent-free cathode production, the carbon, binder, and pore builder are first mixed to a dry powder (e.g., by double blade mill[74]). While with wet coating, porosity is mainly generated by solvent evaporation, dry coating requires a dedicated pore builder (e.g., ammonium bicarbonate). Second, the dry powder is electrostatically charged and sprayed on one side of the grounded current collector by powder guns[72,75]. Third, the cathode is compressed, and the binder is thermally activated by a hot-rolling process[72] before the cathodes are slit.

For solvent-free electrode production, there are, besides the described electrostatic spraying, well-known alternatives such as vapour deposition (e.g., by pulsed-laser or sputtering[76,77]) or reactive mixing and rolling. Vapour deposition has disadvantages compared to electrostatic spraying due to higher working temperatures and slower deposition rates[78], which results in higher costs for large scale manufacturing. Reactive mixing and rolling are a promising alternative for technologies that use structured collector foils (e.g., LABs), which is mandatory for attachment of active material and collector foil in this production concept.

Cell production:

Cell production of LIBs and SIBs entails the same process steps. However, the specific process depends on the choice of cell design: cylindrical cell, prismatic cell or pouch cell. Generally, three prevailing production techniques exist to build the anode-separator-cathode stack: winding, single sheet stacking and z-folding[79]. During winding, anodes, cathodes and separators are provided as endless bands and wrapped together[80]. This process is highly productive, precise and typically used for cylindrical cells and prismatic cells[35,81]. However, the bending stress of the electrodes, which increases by electrode thickness, limits the cell size and energy density[35,80]. Within single sheet stacking, anodes, cathodes, and separators are cut into single sheets and stacked separately[80]. By this technique the mechanical load on the single electrode sheets is uniform and no bending stress occurs, which allows thicker electrodes (>100 µm), resulting in higher energy densities[35]. As the sheets are stacked separately, single sheet stacking is less productive than winding and there is an increased risk of short circuits, due to physical contact of slipped electrodes[35]. During z-folding, which is a state-of-the-art process for pouch cells produced at large scale, anodes and cathodes are first cut into single sheets, typically using a stamping process[82]. Second, the separator is fed as an endless, folded band, and the anodes and cathodes are alternately inserted into the interstitial space[80]. By this technique, electrode thicknesses are not limited by bending stress and the endless separator hinders short circuits by connection of two electrodes[35].

After conducting one of this process alternatives, internal contacts between anode, cathode, and separator assembly are typically created by ultrasonic welding[35,83]. Subsequently, the assembly is inserted into the housing (e.g., aluminium housing for cylindrical and prismatic cells or aluminium–polymer foils for pouch cells). After insertion, the cell is filled with liquid electrolyte under weak vacuum (<300 mbar below ambient pressure) and sealed[84,85], while alternating pressure conditions can reduce the filling time of the liquid electrolyte. The filling process for LIBs, SIBs, LSBs, and LABs is executed using identical technology, but the amount of electrolyte differs (i.e., electrolyte to active material ratio) due to differences in amount, porosity, and reaction pathways of the active materials.

The major difference between LIBs and SIBs compared to LSBs, SSBs and LABs lies in the use of a lithium metal anode for the latter. Due to adhesive properties of lithium[51], laser welding is mandatory for cutting the roll to single sheets. Novel stacking and contacting processes are needed to handle the thin, sticky, and reactive lithium metal sheet. For stacking, the vacuum grippers currently used (for LIBs) to pick and place the electrodes within single sheet stacking and z-folding[82] are not suitable for LSBs, SSBs, and LABs, due to the high risk of damaging the lithium metal foil. Using optimized versions of existing insertion process technologies[86] is more promising for lithium metal foil stacking. However, currently reported stacking speeds of more than 200 sheets per minute[87] will only be hard to reach due to lack of mechanical robustness and the sticky and adhesive nature of the lithium metal sheet.

For consecutive contacting, laser welding is mandatory. Ultrasonic welding is not usable as it relies on mechanical vibrational energy[88], which would damage the thin foil.

In SSBs, no separator foil is used, and the ceramic SEs (sulfidic and oxidic) tend to break upon compressive stress, which means z-folding and winding are not suitable[80,89]. Thus, single sheet stacking is mandatory to build the anode, cathode, and SE stack. The damage-free handling of the adhesive thin lithium metal foil will be challenging within this process step[10]. For sulfidic SSBs, the interface between SE layer and anode needs to be contacted by mechanical pressure after stacking or contacting[10,90]. Compared to LIBs, this new process step is necessary as the SE and the anode must be closely contacted to ensure charge transfer. Therefore, high-quality pressing with optimal pressure, cycle time, and temperature is mandatory. When pressing the stack, there is the risk that individual layers misalign, potentially causing an internal short circuit and possible thermal runaway. To avoid this, the cathode-electrolyte sheet is typically geometrically oversized in SSBs. On the contrary, in LIBs, separator and anode are area-oversized to avoid short circuits and/or lithium deposition. Due to the use of lithium metal at the anode and the availability of electrolyte, the cell is activated and charged after stacking[10]. As the cell is not yet surrounded by housing in this process step, there is a high risk for short circuits, which must be addressed by safety precautions within the production process. After contacting the cell in a next step, it is inserted into a housing and completely closed. The process step filling can be omitted, as electrolyte is already present.

As LABs require a cell design, which allows an external supply of oxygen at the cathode and oxygen protection of the anode, cell assembly differs from that of LIBs, SIBs, LSBs, and SSBs. The stacks consist of an anode, separator, and cathode, as well as a gas diffusion layer (GDL) for oxygen distribution[13,30]. Similar to the z-folding used in LIBs, the separator is fed endlessly and folded in zigzag shape. On the one side, lithium metal anodes and, on the other side, cathodes with GDL between them are inserted. Subsequently, the full stack is inserted in a housing that enables oxygen supply at the cathode side and prevents oxygen from entering the anode side. Consecutively, the housing is filled with electrolyte and closed by welding (e.g., laser or ultrasonic). However, due to these fundamental design differences, it must be assumed that the assembly of LABs will require completely new manufacturing machines.

Cell conditioning: Cell conditioning for LIBs, SIBs, LSBs and LABs begins with the formation process, during which the cell is charged and discharged several times under specific conditions to form the solid electrolyte interphase (SEI)[91,92], which protects anode from adverse ongoing parasitic reactions with electrolyte[93–96]. Gas generated during SEI formation within the cell must be removed prior sealing. Due to the optimization of the formation protocols, including specific current rates, number of charging cycles, resting times and temperature profiles, nowadays it seems to feasible to conduct this procedure for LIBs within less than 20 hours[97,98]. During this procedure, LIBs and SIBs start with a charging step, as all lithium is stored within the cathode in the assembled state. In the case of LSBs and LABs, which are assembled in their charged state, all available lithium is initially located at the anode side. Hence, the already charged LSBs and LABs are activated by filling with electrolyte and the SEI formation starts instantly due to high reactivity of lithium metal. However, a controlled formation procedure is nevertheless conducted to optimize SEI formation.

For SSBs (lithium metal based), a typical formation process is not necessary if optimal SE are used that are stable against lithium metal[99]. In case this concept cannot be materialized, a protective interlayer is necessary. If a concept is targeted to produce this interlayer in situ, a formation process is necessary.

It is crucial to suppress gas generation during this procedure, which would negatively affect the compressed SE and lithium metal interface[63].

After formation, cells are aged and quality control is conducted. Therefore, the cells are stored for two to three weeks and the cell voltage is permanently measured to detect production errors and short circuits that could cause voltage loss[35,100,101].

Implications for process costs

Process steps as well as the technologies, rates and environments for manufacturing of the described battery technologies differ vastly. These differences have significant implications on processing costs and must thus be considered to holistically evaluate competitiveness of these technologies. In the following, the main effects to be considered are listed. LABs are excluded from this analysis, as their technological maturity is currently too low for a reliable large-scale oriented process cost assessment.

With regard to SIBs, process steps and manufacturing technologies are identical to those of LIBs. Nevertheless, due to lower energy densities resulting from lower cell voltage and lower charge densities of anode active material [5], more cells (assuming identical geometry) must be manufactured for the same amount of energy (in kWh) stored. This would increase process costs, as more machines are required, which must be purchased, installed, and operated. Hence, a process cost increase of roughly 15% has been reported[5]. As additional costs, resulting from these increased material quantities, occur along the whole battery value chain (battery material and component production, cell production, module production, and system production), there is currently an uncertainty whether the lower raw material cost of battery grade sodium salts (e.g., Na_2CO_3, cost 0.5 US$ kg^{-1} [5]) compared to battery grade lithium (Li_2CO_3 costs 11 US$ kg^{-1} [102]) can be transformed into lower battery costs.

Regarding LSBs, SSBs and LABs, fewer cells (assuming identical geometry) must be manufactured compared to LIBs for the same amount of energy (in kWh) stored, due to a more optimal parameter set of cell voltage and active material specifications. Nevertheless, compared to LIBs, there are new process specifications that must be considered. For all technologies using a lithium metal foil, anode process cost will be more crucial. Estimated process costs in the range of 300-400 US$ kg^{-1} have been previously reported.[14]

As described, implications by the use of lithium metal are not only limited to its initial production. Additional effects occur within the singling to sheets (slitting and cutting) and the assembly of the sheets within the process step stacking. For singling, machines relying on mechanical force can, in contrary to LIBs, not be used and must thus be replaced by laser machines. While laser cutting promises advantages in cutting quality and maintenance, there are drawbacks in total costs resulting from reduced machine capacities and/or increased machine costs (see Table 3).

With regard to the process step stacking, highly automated processes have been implemented for LIBs, reaching pick and place speeds more than 200 sheets min^{-1} [87]. However, such a high automation rate will be hard to exceed within a lithium metal stacking operation. As stacking is already a cost driver within LIB production (process cost share 11-22%[103]), the process development for lithium metal foil stacking can be assumed to be of crucial relevance from a cost perspective.

On the contrary, anode-free concepts, in which the lithium metal anode is generated in situ, promise process cost advantages, as active material-related anode production steps, which cause process costs of 12-18% even within LIB production[103], could be completely omitted.

For SSBs, in addition to the effects resulting from the use of lithium metal anode, further process differences compared to LIBs must be considered from a cost perspective: The production process for both sulfidic and oxidic SSBs require new process steps, while compared to LIB, other steps can be omitted. Due to the use of a composite cathode, an additional mixing step is necessary. This requirement is crucial from a cost perspective, as the single cathode mixing LIB production already reaches a process cost share of 6-12% [103]. In addition, sulfidic SSBs so far require the additional process step pressing. Estimation of accurate costs for this process step is difficult as such machinery has not yet been developed. However, due to necessary operating accuracy, high automation level, and novelty, its development will require a high effort, which will be allocated in battery costs. Oxidic SSBs require the additional process steps sintering, aerosol deposition, and tempering. Sintering requires the use of permanently operating ovens, which are widely commercially available. When looking at the specifications of these machines, the cost relevance of this new process step becomes obvious: Such ovens reach operating widths of >2 meters, operating lengths of >100 meters, consume several thousand kilowatt-hours of energy (normally gas) and require investments of more than 10 million US$ per machine. Likewise, also tempering significantly contributes to processing costs[104], although it can be conducted at lower temperatures and with reduced cycle times due to the usage of aerosol deposition[67].

In contrast to this crucial process cost effects within SSB production, there are some cost-driving process steps related to LIB that can be completely omitted, namely the liquid electrolyte filling process the formation process step, which account for 5-10% and 8-25% of LIB process costs, respectively[103].

Beside effects resulting from processual changes, requirements concerning manufacturing environments influence costs. Hereby, dry room environments are used when reduced moisture contents in atmosphere are required (<100 ppm of H_2O)[60]. Inert gas atmospheres (such as argon)[10] are used to hinder reaction of battery components with components of ambient air. Within LIB manufacturing, process steps associated with cell production (25-31% of total floor space) are conducted within dry room atmosphere, where inert gas atmosphere is not required. With regard to PLIBs, additional process steps associated with lithium metal production, composite cathode production (sulfidic SSBs) and LAB cathode production must be additionally conducted within dry room or even inert gas atmosphere (see Fig. 3). This will cause additional costs due to the investments in infrastructure and its operation (see Table 4). Cost drivers related to dry room environment are especially the purchase and operation of electricity consuming coolers and blowers[60]. Within inert gas atmosphere, the investments in the housings and the gas purifiers are significant. Compensation of inert gas losses (~0.05 vol%) must be considered during operation[104].

Conclusion and future perspective

Based on the results of Fig. 3, it can be derived that the manufacturing process steps of SIBs are basically identical to those of LIBs, while the process steps of the alternative technologies are to a certain extent similar to those of LIBs. Thus, for the industrialization especially of LSBs, SSBs and LABs, intensive research and development activities focussing on the build-up of new manufacturing competencies and the development of new machinery are necessary. In addition, challenges concerning material composition and cell design must be addressed as PLIBs must compete comprehensively in terms of all key performance parameters (energy, power, safety, life and cost) with the currently dominant LIB to become an alternative in the mass market. Considering the technical challenges PLIBs are facing, it remains to be seen, whether and when one of the discussed, or another

new battery technology is going to contend the currently dominant LIB. However, with view on the currently scheduled production capacities for LIBs, a challenging battery cell technology would need to exhibit significant advantages to justify the billion-dollar investments in new machinery.

References

1. Placke, T., Kloepsch, R., Dühnen, S. & Winter, M. Lithium ion, lithium metal, and alternative rechargeable battery technologies: the odyssey for high energy density. *J. Solid State Electrochem.* **21**, 1939–1964 (2017).

   This article comprehensively reviews the history of battery technologies and offers perspectives of lithium-ion and post lithium ion batteries.

2. Winter, M., Barnett, B. & Xu, K. Before Li Ion Batteries. *Chem. Rev.* **118**, 11433–11456 (2018).

3. Duffner, F., Wentker, M., Greenwood, M. & Leker, J. Battery cost modeling: A review and directions for future research. *Renew. Sustain. Energy Rev.* **127**, 109872 (2020).

   An in-depth analysis of battery cost modelling literature, analyzing them based on various charaterisitcs and identifying a trend towards state-of-the art cell costs between 100 USD kWh^{-1} and 150 USD kWh^{-1}.

4. Pillot, C. *The Rechargeable Battery Market and Main Trends 2017-2030.* (2019).

5. Vaalma, C., Buchholz, D., Weil, M. & Passerini, S. A cost and resource analysis of sodium-ion batteries. *Nat. Rev. Mater.* **3**, 18013 (2018).

   An in-depth overview of SIBs, analyzing the material and production properties and quantifying their implications on costs and cell performance.

6. Gallagher, K. G. *et al.* Quantifying the promise of lithium–air batteries for electric vehicles. *Energy Environ. Sci.* **7**, 1555 (2014).

7. Hagen, M. *et al.* Lithium-Sulfur Cells: The Gap between the State-of-the-Art and the Requirements for High Energy Battery Cells. *Adv. Energy Mater.* **5**, 1401986 (2015).

8. Schnell, J. *et al.* Prospects of production technologies and manufacturing costs of oxide-based all-solid-state lithium batteries. *Energy Environ. Sci.* **12**, 1818–1833 (2019).

   This article evaluates and identifies production technologies for oxidic SSBs, focussing on ceramic processing technologies which are mandatory to produce SEs and composite cathodes.

9. *Mineral Commodity Summaries 2018, (US Department of the Interior, US Geological Survey, 2018)*.

10. Schnell, J. *et al.* All-solid-state lithium-ion and lithium metal batteries – paving the way to large-scale production. *J. Power Sources* **382**, 160–175 (2018).

11. Nanda, S., Gupta, A. & Manthiram, A. Anode-Free Full Cells : A Pathway to High-Energy Density Lithium-Metal Batteries. **2000804**, 1–18 (2020).

12. Randau, S. *et al.* Benchmarking the performance of all-solid-state lithium batteries. *Nat. Energy* **5**, 259–270 (2020).

    In-depth benchmarking analysis of literature-reported all-solid-state-battery performance

data in various configurations.

13. Park, J. O. *et al.* A 1000 Wh kg−1 Li–Air battery: Cell design and performance. *J. Power Sources* **419**, 112–118 (2019).

14. Schmuch, R., Wagner, R., Hörpel, G., Placke, T. & Winter, M. Materials for Automotive Batteries : Perspective on Performance and Cost of Lithium-Based Rechargeable Batteries. *Nat. Energy* **3**, (2018).

Review on current and future materials for automotive batteries with regard to their production as well as performance and cost.

15. Arinicheva, Y. *et al.* Ceramics for electrochemical storage. in *Advanced Ceramics for Energy Conversion and Storage* 549–709 (Elsevier, 2020).

16. Andre, D., Hain, H., Lamp, P., Maglia, F. & Stiaszny, B. Future high-energy density anode materials from an automotive application perspective. *J. Mater. Chem. A* **5**, 17174–17198 (2017).

17. Myung, S. T. *et al.* Nickel-Rich Layered Cathode Materials for Automotive Lithium-Ion Batteries: Achievements and Perspectives. *ACS Energy Lett.* **2**, 196–223 (2017).

18. Scrosati, B., Garche, J. & Tillmetz, W. *Advances in Battery Technologies for Electric Vehicles*. (Elsevier, 2015).

19. Blomgren, G. E. The Development and Future of Lithium Ion Batteries. *J. Electrochem. Soc.* **164**, A5019–A5025 (2017).

20. Lee, H., Yanilmaz, M., Toprakci, O., Fu, K. & Zhang, X. A review of recent developments in membrane separators for rechargeable lithium-ion batteries. *Energy Environ. Sci.* **7**, 3857–3886 (2014).

21. Nayak, P. K., Yang, L., Brehm, W. & Adelhelm, P. From Lithium-Ion to Sodium-Ion Batteries: Advantages, Challenges, and Surprises. *Angew. Chemie Int. Ed.* **57**, 102–120 (2018).

22. Adelhelm, P. *et al.* From lithium to sodium: cell chemistry of room temperature sodium–air and sodium–sulfur batteries. *Beilstein J. Nanotechnol.* **6**, 1016–1055 (2015).

23. Pang, Q., Liang, X., Kwok, C. Y. & Nazar, L. F. Advances in lithium-sulfur batteries based on multifunctional cathodes and electrolytes. *Nat. Energy* **1**, 1–11 (2016).

24. Betz, J. *et al.* Theoretical versus Practical Energy: A Plea for More Transparency in the Energy Calculation of Different Rechargeable Battery Systems. *Adv. Energy Mater.* **9**, 1803170 (2019).

25. Janek, J. & Zeier, W. G. A solid future for battery development. *Nat. Energy* **1**, 1–4 (2016).

26. Bachman, J. C. *et al.* Inorganic Solid-State Electrolytes for Lithium Batteries: Mechanisms and Properties Governing Ion Conduction. *Chem. Rev.* **116**, 140–162 (2016).

27. Famprikis, T., Canepa, P., Dawson, J. A., Islam, M. S. & Masquelier, C. Fundamentals of inorganic solid-state electrolytes for batteries. *Nat. Mater.* **18**, 1278–1291 (2019).

28. Takada, K. Progress in solid electrolytes toward realizing solid-state lithium batteries. *J. Power Sources* **394**, 74–85 (2018).

29. Gallagher, K. G. *et al.* Quantifying the promise of lithium–air batteries for electric vehicles.

Energy Environ. Sci. **7**, 1555 (2014).

30. Bruce, P. G., Freunberger, S. A., Hardwick, L. J. & Tarascon, J.-M. Li–O_2 and Li–S batteries with high energy storage. *Nat. Mater.* **11**, 19–29 (2012).

This review provides a comprehensive technological overview of LSBs and LABs and presents the main challenges to be overcome to use these technologies in mass applications.

31. Choi, J. W. & Aurbach, D. Promise and reality of post-lithium-ion batteries with high energy densities. *Nat. Rev. Mater.* **1**, (2016).

32. Mizuno, F., Nakanishi, S., Kotani, Y., Yokoishi, S. & Iba, H. Rechargeable Li-Air Batteries with Carbonate-Based Liquid Electrolytes. *Electrochemistry* **78**, 403–405 (2010).

33. Liu, Q.-C. *et al.* A Flexible and Wearable Lithium-Oxygen Battery with Record Energy Density achieved by the Interlaced Architecture inspired by Bamboo Slips. *Adv. Mater.* **28**, 8413–8418 (2016).

34. Asadi, M. *et al.* A lithium-oxygen battery with a long cycle life in an air-like atmosphere. *Nature* **555**, 502–506 (2018).

35. Kwade, A. *et al.* Current status and challenges for automotive battery production technologies. *Nat. Energy* **3**, 290–300 (2018).

This article offers an in-depth description of lithium-ion production steps focussing on technical properties, production costs, sale-up issues, and future process innovations.

36. Turetskyy, A. *et al.* Toward Data-Driven Applications in Lithium-Ion Battery Cell Manufacturing. *Energy Technol.* **8**, 1900136 (2020).

37. Dreger, H., Bockholt, H., Haselrieder, W. & Kwade, A. Discontinuous and Continuous Processing of Low-Solvent Battery Slurries for Lithium Nickel Cobalt Manganese Oxide Electrodes. *J. Electron. Mater.* **44**, 4434–4443 (2015).

38. Efficient battery electrode slurry production (Bühler Group, 2017).

39. Zhang, Z., Zeng, T., Lai, Y., Jia, M. & Li, J. A comparative study of different binders and their effects on electrochemical properties of $LiMn_2O_4$ cathode in lithium ion batteries. *J. Power Sources* **247**, 1–8 (2014).

40. Rollag, K., Juarez-Robles, D., Du, Z., Wood, D. L. & Mukherjee, P. P. Drying Temperature and Capillarity-Driven Crack Formation in Aqueous Processing of Li-Ion Battery Electrodes. *ACS Appl. Energy Mater.* **2**, 4464–4476 (2019).

41. Hawley, W. B. & Li, J. Electrode manufacturing for lithium-ion batteries—Analysis of current and next generation processing. *J. Energy Storage* **25**, 100862 (2019).

42. Flynn, J. C. & Marsh, C. Development and experimental results of continuous coating technology for lithium-ion electrodes. in *Thirteenth Annual Battery Conference on Applications and Advances. Proceedings of the Conference* 81–84 (IEEE). doi:10.1109/BCAA.1998.653845

43. Song, Z. *et al.* Origami lithium-ion batteries. *Nat. Commun.* **5**, 3140 (2014).

44. Schmitt, M., Scharfer, P. & Schabel, W. Slot die coating of lithium-ion battery electrodes:

Investigations on edge effect issues for stripe and pattern coatings. *J. Coatings Technol. Res.* **11**, 57–63 (2014).

45. Carvalho, M. S. & Kheshgi, H. S. Low-flow limit in slot coating: Theory and experiments. *AIChE J.* **46**, 1907–1917 (2000).

46. Romero, O. J., Suszynski, W. J., Scriven, L. E. & Carvalho, M. S. Low-flow limit in slot coating of dilute solutions of high molecular weight polymer. *J. Nonnewton. Fluid Mech.* **118**, 137–156 (2004).

47. Jaiser, S., Friske, A., Baunach, M., Scharfer, P. & Schabel, W. Development of a three-stage drying profile based on characteristic drying stages for lithium-ion battery anodes. *Dry. Technol.* **35**, 1266–1275 (2017).

48. Jiang, Z., Zhao, F., Guan, Y. & Qiu, Z. Research on vacuum drying process and internal heat conduction of Li-ion battery core. *Theor. Appl. Mech. Lett.* **9**, 120–129 (2019).

49. Meyer, C., Bockholt, H., Haselrieder, W. & Kwade, A. Characterization of the calendering process for compaction of electrodes for lithium-ion batteries. *J. Mater. Process. Technol.* **249**, 172–178 (2017).

50. Takeda, O. *et al.* Electrowinning of Lithium from LiOH in Molten Chloride. *J. Electrochem. Soc.* **161**, D820–D823 (2014).

51. Meyer, H. C. Some Practical Aspects of Handling Lithium Metal. in 9–15 (1957).

52. Wietelmann, U. Surface-passivated lithium metal and method for the production thereof. US patent 13,515,579 . (2012).

53. Lee, H., Song, J., Kim, Y.-J., Park, J.-K. & Kim, H.-T. Structural modulation of lithium metal-electrolyte interface with three-dimensional metallic interlayer for high-performance lithium metal batteries. *Sci. Rep.* **6**, 30830 (2016).

54. Fu, J. *et al.* In situ formation of a bifunctional interlayer enabled by a conversion reaction to initiatively prevent lithium dendrites in a garnet solid electrolyte. *Energy Environ. Sci.* **12**, 1404–1412 (2019).

55. Tsai, C.-L. *et al.* High conductivity of mixed phase Al-substituted Li7La3Zr2O12. *J. Electroceramics* **35**, 25–32 (2015).

56. Jin, S. *et al.* Solid–Solution-Based Metal Alloy Phase for Highly Reversible Lithium Metal Anode. *J. Am. Chem. Soc.* **142**, 8818–8826 (2020).

57. Qian, J. *et al.* Anode-Free Rechargeable Lithium Metal Batteries. *Adv. Funct. Mater.* **26**, 7094–7102 (2016).

58. Teragawa, S., Aso, K., Tadanaga, K., Hayashi, A. & Tatsumisago, M. Liquid-phase synthesis of a Li3PS4 solid electrolyte using *N*-methylformamide for all-solid-state lithium batteries. *J. Mater. Chem. A* **2**, 5095 (2014).

59. Kotobuki, M., Munakata, H., Kanamura, K., Sato, Y. & Yoshida, T. Compatibility of $Li_7La_3Zr_2O_{12}$ Solid Electrolyte to All-Solid-State Battery Using Li Metal Anode. *J. Electrochem. Soc.* **157**, A1076 (2010).

60. Ahmed, S., Nelson, P. A. & Dees, D. W. Study of a dry room in a battery manufacturing plant

using a process model. *J. Power Sources* **326**, 490–497 (2016).

61. Jung, Y. S., Oh, D. Y., Nam, Y. J. & Park, K. H. Issues and Challenges for Bulk-Type All-Solid-State Rechargeable Lithium Batteries using Sulfide Solid Electrolytes. *Isr. J. Chem.* **55**, 472–485 (2015).

62. Sahu, G. *et al.* Air-stable, high-conduction solid electrolytes of arsenic-substituted Li 4 SnS 4. *Energy Environ. Sci.* **7**, 1053–1058 (2014).

63. Muramatsu, H., Hayashi, A., Ohtomo, T., Hama, S. & Tatsumisago, M. Structural change of Li2S–P2S5 sulfide solid electrolytes in the atmosphere. *Solid State Ionics* **182**, 116–119 (2011).

64. Li, Y., Han, J.-T., Wang, C.-A., Xie, H. & Goodenough, J. B. Optimizing Li+ conductivity in a garnet framework. *J. Mater. Chem.* **22**, 15357 (2012).

65. Miara, L. *et al.* About the Compatibility between High Voltage Spinel Cathode Materials and Solid Oxide Electrolytes as a Function of Temperature. *ACS Appl. Mater. Interfaces* **8**, 26842–26850 (2016).

66. Xia, W. *et al.* Reaction mechanisms of lithium garnet pellets in ambient air: The effect of humidity and CO 2. *J. Am. Ceram. Soc.* **100**, 2832–2839 (2017).

67. Hanft, D., Exner, J. & Moos, R. Thick-films of garnet-type lithium ion conductor prepared by the Aerosol Deposition Method: The role of morphology and annealing treatment on the ionic conductivity. *J. Power Sources* **361**, 61–69 (2017).

68. Schnell, J., Knörzer, H., Imbsweiler, A. J. & Reinhart, G. Solid versus Liquid—A Bottom-Up Calculation Model to Analyze the Manufacturing Cost of Future High-Energy Batteries. *Energy Technol.* **8**, 1901237 (2020).

69. Ma, Z. *et al.* A review of cathode materials and structures for rechargeable lithium-air batteries. *Energy Environ. Sci.* **8**, 2144–2198 (2015).

70. McCloskey, B. D. *et al.* Limitations in Rechargeability of Li-O 2 Batteries and Possible Origins. *J. Phys. Chem. Lett.* **3**, 3043–3047 (2012).

71. Padbury, R. & Zhang, X. Lithium-oxygen batteries - Limiting factors that affect performance. *J. Power Sources* **196**, 4436–4444 (2011).

72. Ludwig, B., Zheng, Z., Shou, W., Wang, Y. & Pan, H. Solvent-Free Manufacturing of Electrodes for Lithium-ion Batteries. *Sci. Rep.* **6**, 23150 (2016).

This paper presents a method for solvent-free electrode production using electrostatic spraying and hot rolling as base for materials dispensing and binder activation.

73. Al-Shroofy, M. *et al.* Solvent-free dry powder coating process for low-cost manufacturing of $LiNi_{1/3}Mn_{1/3}Co_{1/3}O_2$ cathodes in lithium-ion batteries. *J. Power Sources* **352**, 187–193 (2017).

74. Park, D.-W., Cañas, N. A., Wagner, N. & Friedrich, K. A. Novel solvent-free direct coating process for battery electrodes and their electrochemical performance. *J. Power Sources* **306**, 758–763 (2016).

75. Bailey, A. G. The science and technology of electrostatic powder spraying, transport and coating. *J. Electrostat.* **45**, 85–120 (1998).

76. Yan, B., Liu, J., Song, B., Xiao, P. & Lu, L. Li-rich Thin Film Cathode Prepared by Pulsed Laser

Deposition. *Sci. Rep.* **3**, 3332 (2013).

77. Baggetto, L., Unocic, R. R., Dudney, N. J. & Veith, G. M. Fabrication and characterization of Li–Mn–Ni–O sputtered thin film high voltage cathodes for Li-ion batteries. *J. Power Sources* **211**, 108–118 (2012).

78. Koike, S. & Tatsumi, K. Preparation and performances of highly porous layered LiCoO2 films for lithium batteries. *J. Power Sources* **174**, 976–980 (2007).

79. Reinhart, G. *et al.* Research and Demonstration Center for the Production of Large-Area Lithium-Ion Cells. in *Future Trends in Production Engineering* 3–12 (Springer Berlin Heidelberg, 2013).

80. Schilling, A., Schmitt, J., Dietrich, F. & Dröder, K. Analyzing Bending Stresses on Lithium-Ion Battery Cathodes induced by the Assembly Process. *Energy Technol.* **4**, 1502–1508 (2016).

81. Zhang, S. S. A review on the separators of liquid electrolyte Li-ion batteries. *J. Power Sources* **164**, 351–364 (2007).

82. Baumeister, M. & Fleischer, J. Integrated cut and place module for high productive manufacturing of lithium-ion cells. *CIRP Ann.* **63**, 5–8 (2014).

83. Lee, S. S., Kim, T. H., Hu, S. J., Cai, W. W. & Abell, J. A. Joining Technologies for Automotive Lithium-Ion Battery Manufacturing: A Review. in *ASME 2010 International Manufacturing Science and Engineering Conference, Volume 1* 541–549 (ASMEDC, 2010).

84. Günter, F. J. *et al.* Influence of the Cell Format on the Electrolyte Filling Process of Lithium-Ion Cells. *Energy Technol.* ente.201801108 (2019).

85. Günter, F. J., Burgstaller, C., Konwitschny, F. & Reinhart, G. Influence of the Electrolyte Quantity on Lithium-Ion Cells. *J. Electrochem. Soc.* **166**, A1709–A1714 (2019).

86. *Lamination & Stacking of Cells (Manz, 2019)*.

87. Sakti, A., Michalek, J. J., Fuchs, E. R. H. & Whitacre, J. F. A techno-economic analysis and optimization of Li-ion batteries for light-duty passenger vehicle electrification. *J. Power Sources* **273**, 966–980 (2015).

88. Devine, J. Ultrasonic welding. in *ASM Handbook Volume 6: Welding, Brazing, and Soldering* (ed. D.L. Olson, T.A. Siewert, S. Liu, G. R. E.) 324–327 (1993).

89. McGrogan, F. P. *et al.* Compliant Yet Brittle Mechanical Behavior of Li_2S-P_2S_5 Lithium-Ion-Conducting Solid Electrolyte. *Adv. Energy Mater.* **7**, 1602011 (2017).

90. Hao, F., Han, F., Liang, Y., Wang, C. & Yao, Y. Architectural design and fabrication approaches for solid-state batteries. *MRS Bull.* **43**, 775–781 (2018).

91. An, S. J. *et al.* The state of understanding of the lithium-ion-battery graphite solid electrolyte interphase (SEI) and its relationship to formation cycling. *Carbon N. Y.* **105**, 52–76 (2016).

92. Wood, D. L., Li, J. & Daniel, C. Prospects for reducing the processing cost of lithium ion batteries. *J. Power Sources* **275**, 234–242 (2015).

93. Arora, P. Capacity Fade Mechanisms and Side Reactions in Lithium-Ion Batteries. *J. Electrochem. Soc.* **145**, 3647 (1998).

94. Bieker, G., Winter, M. & Bieker, P. Electrochemical in situ investigations of SEI and dendrite formation on the lithium metal anode. *Phys. Chem. Chem. Phys.* **17**, 8670–8679 (2015).

95. Cheng, X.-B. *et al.* A Review of Solid Electrolyte Interphases on Lithium Metal Anode. *Adv. Sci.* **3**, 1500213 (2016).

96. Peled, E. The Electrochemical Behavior of Alkali and Alkaline Earth Metals in Nonaqueous Battery Systems—The Solid Electrolyte Interphase Model. *J. Electrochem. Soc.* **126**, 2047 (1979).

97. Mao, C. *et al.* Balancing formation time and electrochemical performance of high energy lithium-ion batteries. *J. Power Sources* **402**, 107–115 (2018).

98. An, S. J., Li, J., Du, Z., Daniel, C. & Wood, D. L. Fast formation cycling for lithium ion batteries. *J. Power Sources* **342**, 846–852 (2017).

99. Kato, Y. *et al.* High-power all-solid-state batteries using sulfide superionic conductors. *Nat. Energy* **1**, 16030 (2016).

100. Tagawa, K. & Brodd, R. J. Production Processes for Fabrication of Lithium-Ion Batteries. 181–194 (2009). doi:10.1007/978-0-387-34445-4

101. Verma, P., Maire, P. & Novák, P. A review of the features and analyses of the solid electrolyte interphase in Li-ion batteries. *Electrochim. Acta* **55**, 6332–6341 (2010).

102. LME. London metal exchange. (2019). Available at: https://www.lme.com/. (Accessed: 30th January 2020)

103. Duffner, F., Mauler, L., Wentker, M., Winter, M. & Leker, J. Large-scale automotive battery cell manufacturing: Analyzing strategic and operational effects on manufacturing costs using a process-based costing approach. *Intern. J. Prod. Econ.* Accepted Manuscript (2020).

Forecast of large-sclae lithium-ion battery manufcaturing costs based on more than 250 parameters related to technical parameters, product characterisics, operating conditions and factor prices.

104. Schnell, J., Knörzer, H., Imbsweiler, A. J. & Reinhart, G. Solid versus Liquid—A Bottom-Up Calculation Model to Analyze the Manufacturing Cost of Future High-Energy Batteries. *Energy Technol.* **8**, 1901237 (2020).

105. Cano, Z. P. *et al.* Batteries and fuel cells for emerging electric vehicle markets. *Nat. Energy* **3**, 279–289 (2018).

106. Hagen, M. *et al.* Lithium-Sulfur Cells: The Gap between the State-of-the-Art and the Requirements for High Energy Battery Cells. *Adv. Energy Mater.* **5**, (2015).

107. Lee, H. C. *et al.* High-Energy-Density Li-O2 Battery at Cell Scale with Folded Cell Structure. *Joule* **3**, 542–556 (2019).

108. Manthiram, A., Yu, X. & Wang, S. Lithium battery chemistries enabled by solid-state electrolytes. *Nat. Rev. Mater.* **2**, 16103 (2017).

109. Lee, Y.-G. *et al.* High-energy long-cycling all-solid-state lithium metal batteries enabled by silver–carbon composite anodes. *Nat. Energy* (2020). doi:10.1038/s41560-020-0575-z

110. Aurbach, D., McCloskey, B. D., Nazar, L. F. & Bruce, P. G. Advances in understanding

mechanisms underpinning lithium – air batteries. *Nat. Energy* **1**, 1–11 (2016).

111. Vaalma, C., Buchholz, D., Weil, M. & Passerini, S. A cost and resource analysis of sodium-ion batteries - Supplementary Information. (2018).

112. Moores, S. *Dawn of the battery megafactories and the impact on industrial minerals*.

113. Schünemann, J. H. Modell zur Bewertung der Herstellkosten von Lithiumionenbatteriezellen. (PhD Thesis, Technische Universität Braunschweig, 2015).

Acknowledgements

This work was supported by the German ministry of Education and Research (BMBF) through the project ProLiFest (03XP0253A). We acknowledge Mr. Andre Bar for the assistance in preparing Fig. 1-5.

Competing interest

Fabian Duffner and Niklas Kronemeyer are employees at Porsche Consulting GmbH.

Display items

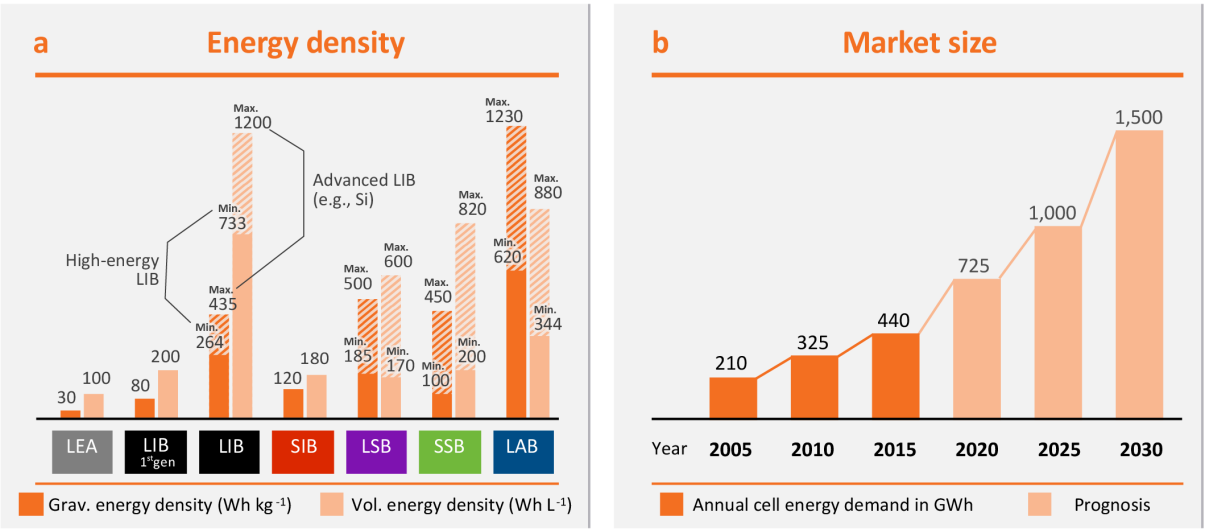

Fig. 1 | Practical technology-specific volumetric and gravimetric energy densities and development of the rechargeable battery market size over time. **a**, Practical volumetric and gravimetric energy densities per technology at cell level: current high-energy LIB cell as minimum and advanced LIB configuration (the latter e.g., using Si-based anode) as maximum value; prototype cell data for SIB, LSB, SSB and LAB with minimum and maximum values given for Li-metal based systems[1,5,12–14,105,106]. **b**, Development of the rechargeable battery market from 2005 to 2030. In 2005, market was dominated by the LEA technology with a production capacity (in GWh) share of more than 80%. This dominant position of LEAs can still be observed in mitigated form with share of more than 60% in 2020. By 2030 LIB becomes the dominant technology with a production capacity share of more than 50%[4]. The past (2005-2015) and prognosis (beyond 2020) data are taken from ref.[4].

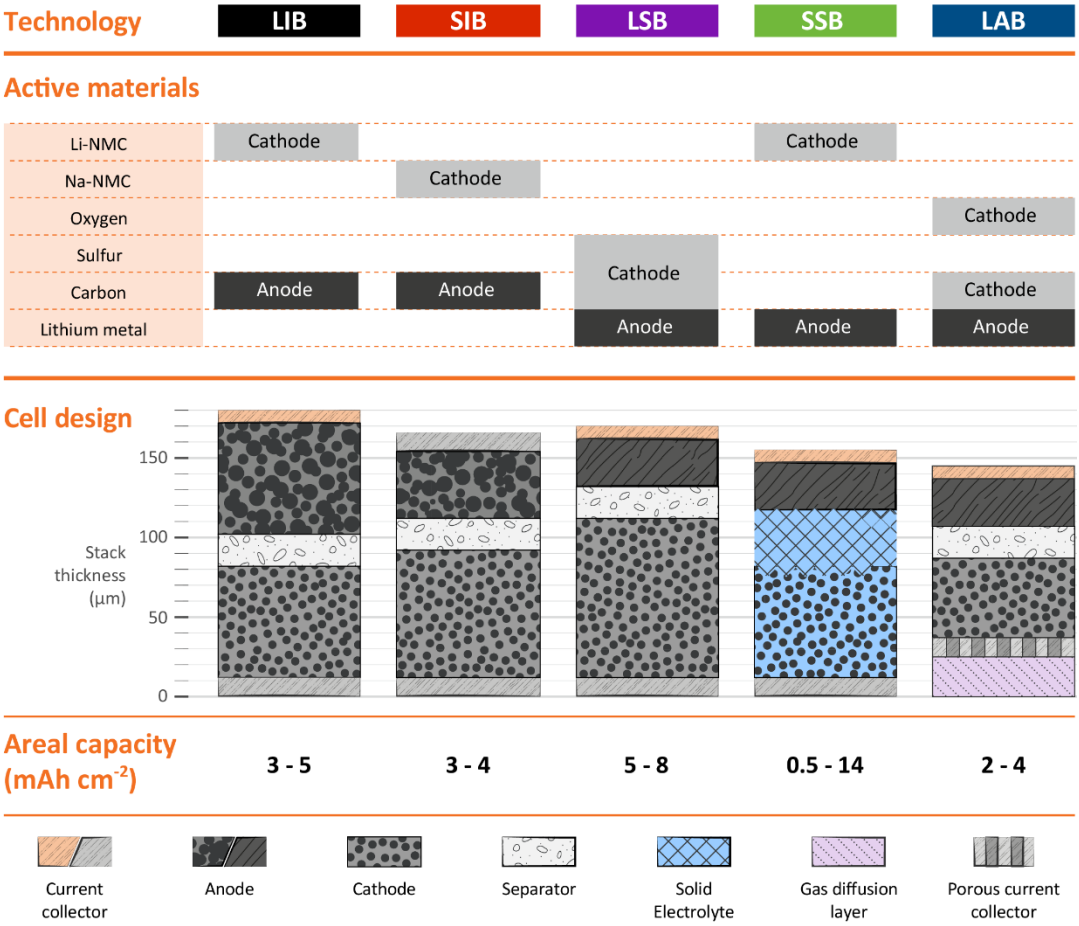

Fig. 2 | Schematic electrode stack design for LIBs, SIBs, LSBs, SSBs and LABs with associated active materials and areal capacity ranges typically used. The orange/grey colour of the current collector correspond to copper and aluminium foil, respectively. The given thicknesses of electrodes and inactive components may not be to scale, as they depend on the chosen cell layout.

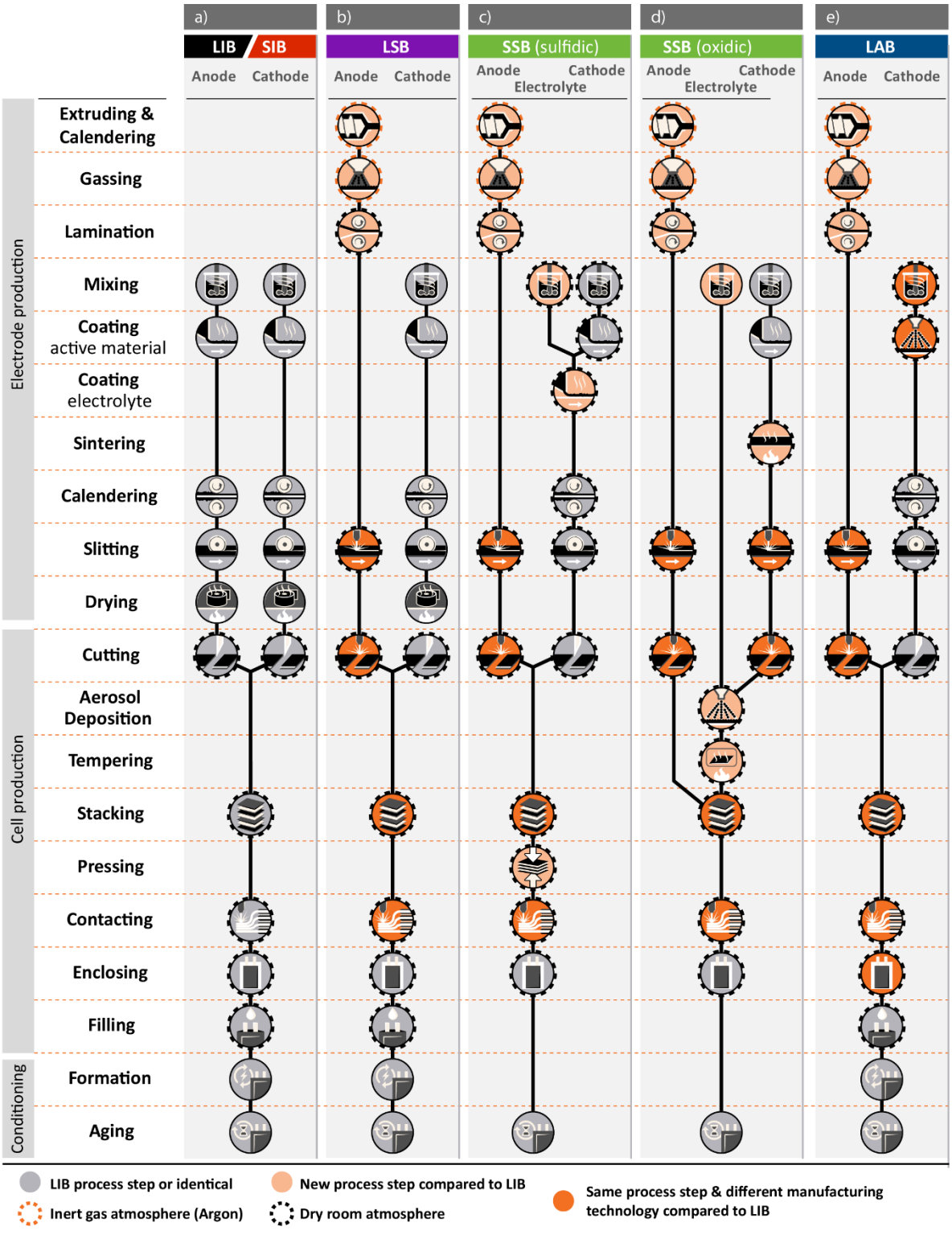

Fig. 3 | Battery cell production chain for selected battery technologies. a, *SIB and LIB production process steps are basically identical. b-e, Anode production steps for LSBs, SSBs, and LABs represent the production of thin lithium-metal foils. Due to properties of the used metallic lithium, anode production must be conducted in inert gas or dry room atmosphere and laser application is mandatory for the process steps cutting, slitting and contacting. Further, for the process step stacking, process technologies must be developed to enable fast handling of ultrathin, sticky and adhesive anode foils. c, for sulfidic SSB cathode production, additional mixing and coating operation is necessary to build the composite cathode layer. Further, cathode production must be conducted within dry room atmosphere to avoid reaction of sulfidic electrolyte with ambient air and*

moisture. Within cell production, the process step pressing is necessary, to contact SE and anode. d, For the production of oxidic SSBs, sintering and tempering operations are necessary due to the brittleness of oxidic SEs. After sintering, production steps must be conducted in dry room atmosphere to prevent degradation of the SE. c-d, For sulfidic and oxidic SSBs, the process steps filling and formation can be omitted, as the electrolyte is already present and the SE is ideally sufficiently stable against lithium. e, For LABs, within cathode production, solvent free production steps which consists of the process steps dry mixing and electrostatic spraying (conducted within dry room atmosphere) are mandatory to avoid moisture, which would reduce the storage capacity of the used carbon at the cathode. Within cell production, the additional GDL within the cell stack and the required cell design, that enables oxygen supply at the cathode and prevents oxygen at the anode side, drives significant adaptions of process steps stacking, contacting and enclosing.

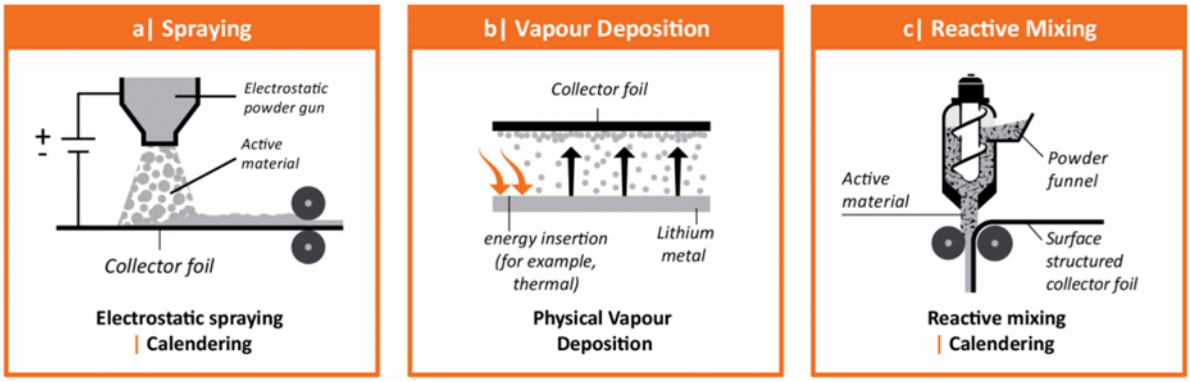

Fig. 4 | Prospective concepts for solvent-free electrode production. a, Pulverised active material is electrostatically charged and sprayed by a powder gun onto a current collector foil. **b,** Active material substrate is transformed from solid state to gas phase by energy insertion (e.g., by sputtering or pulsed-laser) and is thus deposited on the current collector foil. **c,** Pulverised active material is directly spread on collector foil and inserted to calendaring process. Therefore, 3-D structured current collector foil (e.g., grid) is mandatory.

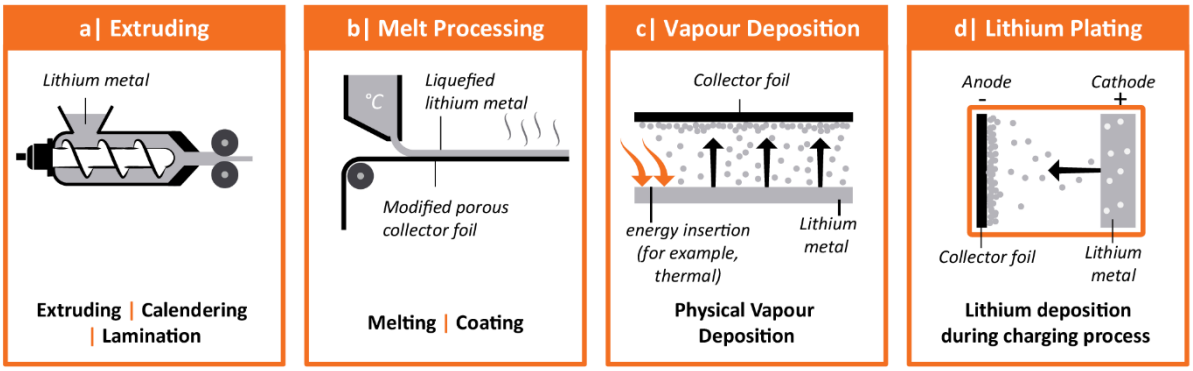

Fig. 5 | Process concepts for lithium metal anode production. a, Lithium metal is extruded into foil shape and compressed by several calendering operations to reduce thickness. Finally, the lithium metal foil is laminated onto a current collector foil. **b,** Lithium metal is liquefied (approx. 180 °C[51]) and coated onto the Cu current collector foil. A porous collector is mandatory for lithium infiltration. **c,** Lithium metal substrate is evaporated by energy insertion (e.g., by sputtering or pulsed-laser) and is thus deposited onto the current collector foil. **d,** Lithium metal is deposited electrochemically from lithium-ions provided by the cathode active material and/or sacrificial salts. Lithium metal anode is formed during the first charge procedure.

Table 1 | Overview of key advantages and disadvantages as well as technical specifications of discussed rechargeable battery technologies. Technical specifications for LIB and PLIB technologies such as nominal voltage, operating voltage window, power at cell level, cycle life, energy efficiency and tendency for self-discharge were taken from literature.[12,105,107–111] Values might deviate individual cases, depending on the used cell chemistry (active material, type of electrolyte, presence of redox mediators in LABs), cell parameters and operating conditions such as temperature; external pressure on stack. ND, no data available; RT, room temperature.

	LIB[105]	**SIB**[111]	**LSB**[105,106]	**SSB**[12,108,109]	**LAB**[105,107,110]
Advantages	High technological maturity High volumetric energy density Long life	Raw material availability	Low cost cathode High gravimetric energy density	Higher safety with Li metal Selected systems with wide temperature range High energy density with Li metal	Low-cost, cathode High theoretical gravimetric energy density
Disadvantages	Costs of selected materials Availability and environmental impact of raw materials	Moderate volumetric and gravimetric energy densities Promising chemistries not finally decided	Large electrolyte excess required Pronounced self-discharge of discharge intermediates High cost anode	May require stack pressure Uncertain material and processing costs High cost anode Promising chemistries not finally decided	Low cycle life Pronounced voltage hysteresis;, poor energy efficiency Sensitive to air impurities High cost anode Promising chemistry not finally decided
Nominal voltage	3.2-3.85 V	3.1-3.3V	2.1-2.2 V	3.7-3.8 V	2.6-2.9 V
Operating voltage window	3.0-4.2 V	1.0-4.2 V	1.8-2.8 V	2.5-4.25 V (often above RT)	2.1-4.3 V
Areal electrode capacity	3-5 mAh cm^{-2}	3-4 mAh cm^{-2}	5-8 mAh cm^{-2}	0.5-14 mAh cm^{-2}	2-4 mAh cm^{-2}
Power (Cell)	1-20 kW kg^{-1}	2-5 kW kg^{-1}	0.1-1 kW kg^{-1}	0.01-3 kW kg^{-1} (temperature-dependent)	ND
Cycle Life	1000-6000	500-4000	100-500	100-1000	5-100
Energy Efficiency	High (>90%)	High (>90%)	Moderate (70-95%)	Low (50-76%)	Low (60-80%)
Self-Discharge	Low	Low-Medium	High	Low	ND

Table 2 | The largest LIB production sites announced for 2025 in Europe, Asia and USA.

Region / Manufacturer	Factory location	Headquarter location	Capacity 2025 (GWh)
Europe			
LG Chem	Wroclaw | Poland	South Korea	62
CATL	Erfurt | Germany	China	37
Northvolt	Skellefteå | Sweden	Sweden/Germany	32
Samsung SDI	Goed | Hungary	Hungary	16
Northvolt/VW	Salzgitter | Germany	Sweden/Germany	16
SK Innovation	Komárom | Hungary	South Korea	10
Asia			
LG Chem	Nanjing (two locations) | China	South Korea	99
CATL	Ningde | China	China	76
Wanxiang (A123)	Hangzhou | China	China	46
Tesla	Shanghai | China	US	26
BYD	Shenzhen | China	China	15
Samsung SDI	Ulsan | South Korea	South Korea	23
Panasonic	Suminoe | Japan	Japan	20
LG Chem	Ochang | South Korea	South Korea	19
USA			
Tesla	Sparks | US	US	76
LG Chem	Holland | US	South Korea	19
SKI	Commerce | US	South Korea	13

Data taken from literature [4,112].

Table 3 | Comparison of singling technologies.

Process step	**Slitting**		**Cutting**	
Process technology	Roll-knife	Laser	Stamping	Laser
Investment per machine	~1 Mio. US$	~2 Mio. US$	~0,5 Mio.US$	~0,5 Mio.US$
Machine capacity	4054 sheets min^{-1}	4054 sheets min^{-1}	288 sheets min^{-1}	102 sheets min^{-1}
Working speed	100 m min^{-1}	100 m min^{-1}	360 strokes min^{-1}	100 m min^{-1}
Working width	1.5 m	1.5 m	-	-

Machine capacities are calculated based on working speed and/or working width, overall equipment effectiveness (80%), sheet width (95 mm), and sheet length (296 mm). For slitting, working speeds are taken from ref. [103,113] and working widths are taken from ref. [35,103]. For cutting, working speeds are taken from ref. [103,113]. Investments for slitting are adopted from ref. [104,113] and for cutting from ref. [103,113].

Table 4 | Comparison of manufacturing environments.

	Standard	**Dry room**	**Inert gas**
Investment	~600 US$ m^{-3}	~2,000 US$ m^{-3}	>13,000 US$ m^{-3}
Resource consumption	-	0.17 US$ m^{-3} d^{-1} (electricity)	2.76 US$ m^{-3} d^{-1} (argon)

Reference parameters: Location Germany; Height factory building 4m; Inert gas atmosphere within glovebox.
Data taken from literature [103,104,113] .